J Comput Aided Mol Des (2006) 20:673–684
DOI 10.1007/s10822-006-9088-5

ORIGINAL PAPER

Molecular dynamics simulation of the human adenosine A_3 receptor: agonist induced conformational changes of Trp243

Christian Hallmen · Michael Wiese

Received: 10 July 2006 / Accepted: 17 October 2006 / Published online: 24 November 2006

Abstract The adenosine A_3 receptor together with rhodopsin belongs to Class A of the G-protein coupled receptors. As the crystal structure of bovine rhodopsin represents the dark (inactive) state of the receptor, the details of GPCR activation are still unknown. In this molecular dynamics study we investigate how the homology model of the human adenosine A_3 receptor responds to ligand exposure. To this end we placed the homology model in a POPC membrane model. After equilibrating for 13 ns an agonist (Cl-IB-MECA) and an inverse agonist (PSB-10) were placed inside the putative binding pocket. In the following 10 ns molecular dynamics simulation we observed a different behaviour of the side-chain torsions of Trp243$^{6.48}$, depending on the presence or absence of the agonist or inverse agonist. This conformational change of Trp243 correlates with the assumed influence of ligands on receptor activation. Other predicted conformational changes of the receptor could not be observed yet. So Trp243 may represent the first switch in receptor activation.

Keywords Adenosine A_3 receptor · GPCR · Molecular dynamics · Phospholipid bilayer · Receptor activation

C. Hallmen (✉) · M. Wiese
Pharmaceutical Institute, University of Bonn, Bonn, Germany
e-mail: challmen@uni-bonn.de

Introduction

Adenosine receptors belong to the super-family of G-Protein coupled receptors (GPCRs). These receptors are the target of approximately 40% of all prescription pharmaceuticals on the market [1]. GPCRs share the common structure of seven transmembrane helices and respond to a wide array of signaling ligands (ions, organic odorants, amines, peptides, proteins, lipids, nucleotides, and even photons). In 2000 the crystal structure of bovine rhodopsin was elucidated by Palczewski et al. [2]. Rhodopsin is still the only GPCR with a 3D-structure available. This structure represents the receptor in its inactive (dark) state. Upon absorption of a photon the covalently bound 11-*cis*-retinal isomerizes to all-*trans*-retinal. This process induces a conformational change of the receptor to form the active meta-II rhodopsin. The rhodopsin crystal structure shows that the TM helices are locked in an inactive conformation by interhelical interactions involving conserved amino acids [3]. The details of the activation process are still unknown, although some experimental results shed light onto this field of research. The first hints came from the discovery that discrete mutations lead to constitutive active mutants (CAMs). Theses CAMs show a dramatically higher activity compared to the basal activity of the wild-type receptors. But the picture this discovery draws is quite hazy. Mutations leading to constitutive activity can be found in nearly any receptor domain, e.g., the second [4] and third [5] extracellular loop and the C-terminal part of the third intracellular loop [6, 7]. These mutations probably disrupt stabilizing interactions in the protein that keep it in the inactive state.

One receptor domain seems to be particularly important for receptor activation within the family A

GPCRs: the highly conserved D/E RY (Glu/Asp–Arg–Tyr) motif. Comparison of wild-type rhodopsin with rhodopsin mutated at Glu134$^{3.49}$ by flash photolysis suggests that proton uptake of Glu134$^{3.49}$ accompanies formation of the metarhodopsin II state [8]. In agreement charge neutralizing mutations of Glu or Asp in this position were found to cause a dramatic increase in constitutive activity [9–11].

Not only substitution of polar amino acids capable of forming hydrogen bonds or salt bridges, but also substitution of lipophilic amino acids may lead to CAMs. Any substitution of Ala$^{6.34}$ in the α_{1b}-adrenoceptor caused increased agonist-independent receptor activity [7]. And nearly any substitution of Met257$^{6.40}$ (except for leucine) in rhodopsin leads to significant constitutive activity [12].

Some conformational changes involved in the receptor activation have been identified. Application of the substituted cysteine accessibility method to a constitutively active β2 adrenergic receptor showed that a cysteine in TM6 became accessible in the binding crevice to a charged, sulfhydryl-reactive reagent [13]. This observation indicates a counter-clockwise rotation (as viewed from the extracellular side) or tilting of the helix in this CAM. Cross-linking pairs of histidines with Zn^{2+} prevented transducin activation, providing indirect evidence that movements of these two domains are important for activation.

Site-directed labelling of single cysteines inserted at the cytoplasmic side of the transmembrane helices of rhodopsin with sulfhydryl-specific nitroxide spin labels indicates movements of the cytoplasmic end of TM6 upon light-induced activation of rhodopsin [14].

In case of rhodopsin, the covalently bound 11-*cis*-retinal acts like an inverse agonist and stabilizes the inactive conformation. Patel et al. used high-resolution solid-state NMR measurements to show that the retinal translates toward TM5 upon conversion to the active intermediate metarhodopsin II. Retinal isomerization results in a large rotation of the C20 methyl group toward the second extracellular loop (EL2) rather than in a large displacement of the ionone ring toward TM3 or TM6 [15].

Trp265$^{6.48}$ lies within the arc created by the 11-*cis* retinal and the Lys296 side-chain. Retinal analogs that lack the bulky ionone ring are not able to activate rhodopsin [16]. Patel et al. conclude that Trp265$^{6.48}$ is the only amino acid in the retinal binding pocket that restricts retinal translation [15].

Translation of the retinal toward TM5 would result in outward rotation of TM6 by direct interaction between the tryptophan side-chain and either the Lys296 or Ala295 side chains. Mutation of Trp265$^{6.48}$ to alanine decreased the activity of rhodopsin significantly [17]. Electron crystallography revealed that metarhodopsin I formation does not involve large rigid-body movements of helices, but a rearrangement in the region of Trp265 [18].

The amino acid corresponding to Trp265 in bovine rhodopsin is Trp243 in the human adenosine A_3 receptor (hA_3-receptor). Mutation of this amino acid to alanine had an interesting effect on receptor activation. Though agonists had an affinity similar to the wild-type receptor, they failed to activate the W243A mutant receptor [19], pointing to the importance of this residue for receptor activation. Therefore we focused our attention in this molecular dynamics study on this amino acid.

Material and methods

Lipids

As a starting point we took a bilayer consisting of a 1-palmitoyl-2-oleoyl-glycerophosphocholine (POPC) patch including initially 96 lipids and 7TM-Alamethicin (http://www.ucalgary.ca/~tieleman/files/almN7end.pdb). The topology file for the POPC molecule was available from http://www.ucalgary.ca/~tieleman/files/popc.itp

Protein

The molecular model of the hA_3-receptor was built using the homology model tool of MOE 2003.02. The X-ray structure of bovine rhodopsin (PDB-ID: 1L9H) [20] was used as a structural template. The alignment of the seven transmembrane helices is based on the WHAT-IF Profile V2.0 for class A GPCRs, taken from the GPCRDB database (http://www.gpcr.org/7tm/). Further details are described in [21].

Insertion of the protein into the bilayer and equilibration

Alamethicin was removed and the homology model of hA_3-receptor was placed in the resulting hole. Great care was taken to guarantee that the lipophilic part of the seven TMs were located within the lipophilic central area of the bilayer. Afterwards a thorough examination revealed some POPC molecules that needed to be modified because of close contacts with the protein. Usually small changes in the conformation of the fatty acid chains were sufficient, but in a few cases the whole molecule had to be deleted (87 POPC molecules

remained). Subsequently water and 10 chlorine counter ions were added. Water molecules placed by GROMACS inside the phospholipid membrane were removed manually.

The protein–lipid equilibration was achieved through a three-stage process. First, the system was energy-minimized using the GROMOS force field with position restraints applied to the protein. Energy minimization was initially performed with the steepest descent algorithm (until a gradient of 1,000 kJ mol^{-1} nm^{-1} was reached) and subsequently with the conjugated gradient algorithm (until a gradient of 100 kJ mol^{-1} nm^{-1} was reached). Afterwards the position restraints were removed and the energy-minimization cycle was repeated.

Finally, the system was submitted to a short MD simulation (200 ps), where position restraints were applied to the protein.

MD Calculations

MD simulations were performed with the GROMACS package version 3.2. Simulations were run at a temperature of 310 K and a pressure of 1 bar in an isothermal-isobaric ensemble (NPT) with periodic boundaries present. Both Berendsen temperature and semi-isotropic pressure couplers were chosen to keep these parameters constant. The time step for the simulations was 2 fs. A LINCS algorithm was used to maintain the geometry of the molecules. Long-range electrostatic interactions were calculated with the particle-mesh Ewald (PME) method. PME tends to slow down the computation but increases its quality because it removes any cut-off related electrostatic interaction artefacts. Lennard-Jones interactions were cut off at 2.0 nm. The single-point charge (SPC) water model was used to describe the water in the simulation box.

Ligand structure preparation and docking experiments

Models of adenosine receptor ligands used in this study were constructed using the ''Sketch Molecule'' module of Sybyl 7.0.

The structures were minimized with molecular mechanics (using the Tripos force field, conjugate-gradient minimizing method) and subsequently with the MOPAC software (using the semiempirical AM1 method). Partial atomic charges were also taken from the MOPAC calculation. Automatic docking of the ligands was carried out by the GOLD-Software with standard default settings. The binding pocket for the agonist was defined as being within 14 Å of the sidechain of Ser271, for antagonists as being within 14 Å of the sidechain of Trp243. Up to 30 docking runs per ligand were carried out. An early termination was allowed if the top 3 solutions are within 1.5 Å RMSD. The GOLD-Score was used as the fitness function. Topology-files were created by the PRODRG software [22].

MD Runs

One 23-ns MD simulation was run for the unoccupied receptor. After 13 ns equilibration was reached. At this point a snapshot of the model was taken and the two ligands PSB-10 (inverse agonist) and Cl-IB-MECA (agonist) were placed inside the binding pocket as suggested by docking experiments. Water molecules within 0.2 nm were removed to accommodate the ligands.

Both models were submitted to a 10 ns MD simulation.

Results and discussion

Equilibration of the hA_3 receptor in a phospholipid bilayer

Our aim was to look for differences in the behaviour of the hA_3 receptor model in the presence and absence of an agonist and an antagonist. First we had to ensure equilibration of the receptor model in the bilayer. We took the change of total energy as the main criterion (Fig. 1). The biggest decline in energy occurred during the first nanosecond which can be attributed to the relaxation of the protein after removal of position restraints. Afterwards a period of slow but steady

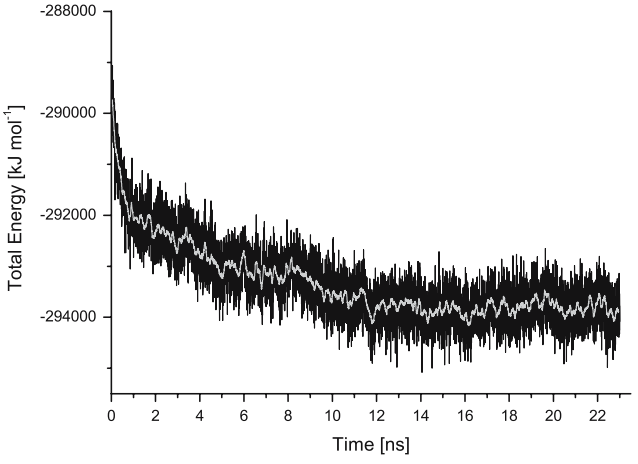

Fig. 1 Total energy plotted versus time. Grey line shows the average energy over 100 ps

decrease in total energy followed. After 13 ns no further change in total energy could be observed. In addition we examined the root mean square deviation (RMSD) of the backbone atoms from the starting position (Fig. 2). After 13 ns no significant change in the RMSD value was observed, neither in the whole protein nor in the TM domains. As expected changes in the TM domains were less pronounced even though least square fitting was performed over the backbone of the whole protein.

An important criterion to judge the quality of the simulation is whether the helical structure of the seven TMs was preserved. Figure 3 shows the fraction of time each amino acid possesses a helical conformation. The eight helical domains of the GPCRs can be identified, although it is not easy to differentiate between TM7 and the intracellular eighth helix.

Prolines produce kinks in α-helices caused by steric clash of the pyrrolidine ring with the backbone and the loss of the hydrogen bonds between the amide nitrogen and the carbonyl at the (i-4) position. In Fig. 3 such prolines cause the observed lack of helical structure in single amino acids within the TM domains. For example Val63 and Trp185 have a helicicity of 19% and 1% caused by Pro67 and Pro189, respectively.

Behaviour of the second extracellular loop

The most obvious change in the receptor conformation occurred in the second extracellular loop (EL2). In the crystal structure of rhodopsin this loop forms a beta sheet and is in close contact with the covalently bonded retinal moiety. But in this conformation EL2 would prevent ligands from reaching the binding pocket.

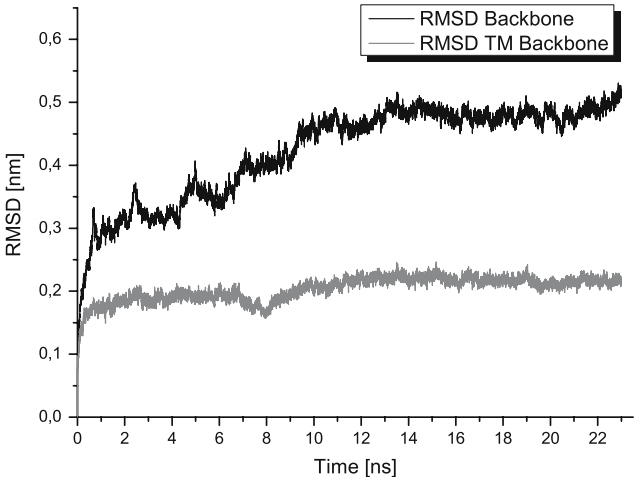

Fig. 2 RMSD of all backbone atoms (black line) or the backbone atoms in the TM region (grey line) plotted versus time

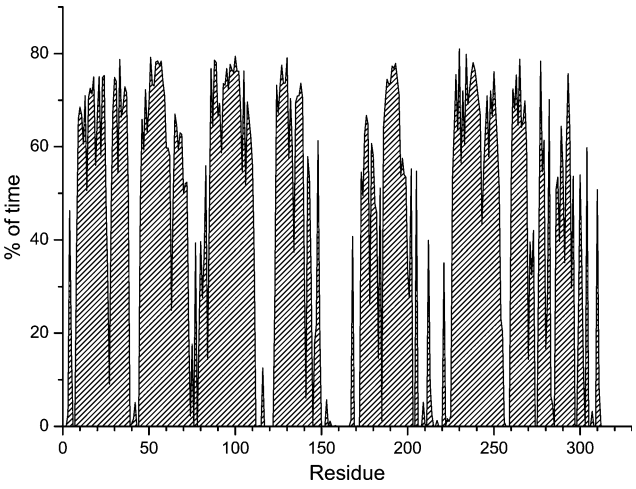

Fig. 3 Helicity of all amino acids measured as the percentage of time phi and psi angles adopt a α-helical conformation

Figure 4 shows the structure of the hA_3 receptor at the beginning of the simulation (left) and after 23 ns (right). Even though the α-helices in the TM domains were preserved the β-sheet was not. In this new conformation EL2 is less of an obstacle for an approaching ligand. After ligand binding EL2 may revert back to the β-sheet structure and thereby prolong the time a ligand spends in the binding pocket. This hypothesis may explain the observed involvement of EL2 in ligand recognition. Kim et al. detected some amino acids in EL2 involved in ligand recognition through site-directed mutagenesis of the human A_{2a} adenosine receptor [23]. Olah et al. constructed chimeric A_1/A_3 receptors and identified the distant 11 amino acids of this loop to be responsible for differences in binding affinities [24]. Regarding the role of EL2 in aminergic GPCRs Shi and Javitch give an overview [25]. For the muscarinic receptors a M2/M5 chimeric receptor and site-directed mutagenesis reveal the involvement of EL2 in allosteric modulation [26, 27]. Allosteric modulators with positive cooperation may bind to EL2 with β-sheet conformation and thereby stabilize this conformation which in turn keeps the orthoster in the binding site. Following this theory allosteric modulators with negative cooperation may bind to EL2 without β-sheet conformation and thereby prevent the EL2 from stabilizing the ligand binding.

Placement of the ligands in the binding pocket

Our aim was to investigate the behaviour of the receptor in the presence of ligands. Therefore we chose an agonist (Cl-IB-MECA) [28] and an inverse agonist (PSB-10) [29], instead of an antagonist, in order to

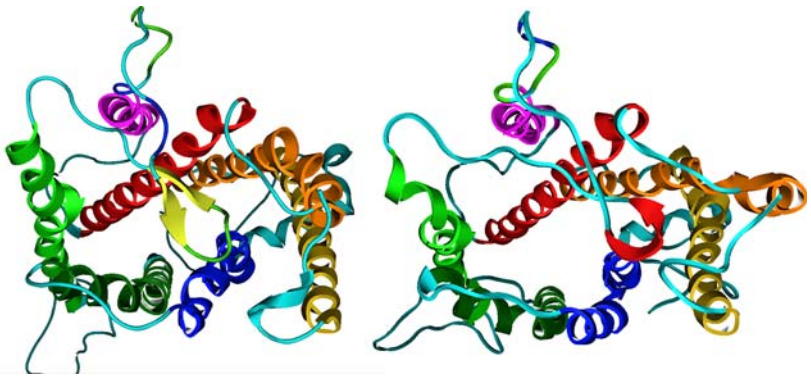

Fig. 4 Protein backbone viewed from the extracellular side before (left side) and after 23 ns of simulation (right side). (Colour-coding: TM1: dark yellow, TM2: orange, TM3: dark red, TM4: magenta, TM5: light green, TM6: dark green, TM7 dark blue, β-sheet: yellow)

maximize the differences that may be observed. Figure 5 shows the chemical structures of both ligands.

PSB-10 was docked into the homology model of the hA_3 receptor derived from the crystal structure of bovine rhodopsin. Figure 6 shows the docking result for this ligand. Potential hydrogen bonds are with Asn250 (TM6) and Ser165 (EL2) otherwise the high affinity of PSB-10 can be attributed to the lipophilic trichlorophenyl moiety which perfectly fits into the lipophilic part of the binding pocket.

Cl-IB-MECA was docked into a modified receptor model. Based on the results from mutagenesis study of the hA_3 receptor by Gao et al. [19] we built the putative active conformation of the hA_3-receptor by modifying the conformation of Trp243 ($\chi1$ from –65° to 174° and $\chi2$ from –79° to –96°). Through this modification a polar area near Ser271 becomes accessible to a ligand more easily. We used this receptor model successfully to dock agonists and partial agonists in the putative binding pocket [21]. Recently, Kim et al. successfully used a similarly modified receptor model in docking studies [30]. Figure 7 shows the docking result for Cl-IB-MECA. Several hydrogen bonds between the agonist and the protein seem to exist. They are established mainly by the modified ribose moiety. Partners for hydrogen bonding include the backbone carbonyl of Leu90 (TM3), Thr94 (TM3), Trp243 (TM6), Asn250 (TM6), Ser271 (TM7) and Asn274 (TM7).

Based on these docking results we placed these ligands individually in the binding pocket of the receptor obtained after 13 ns of equilibration. The resulting structures were submitted for another 10 ns of molecular dynamics simulation.

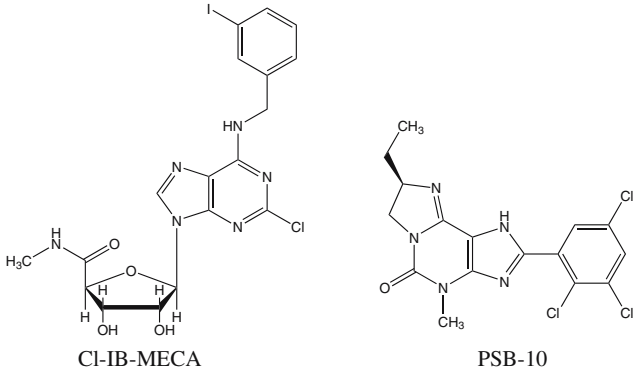

Fig. 5 Chemical structures of the agonist IB-MECA and the inverse agonist PSB-10

Conformational changes in Trp243$^{6.48}$

As described above, Trp243$^{6.48}$ is assumed to be involved in receptor activation. Therefore we focused our attention on conformational changes of this amino acid. Figure 8 shows the torsional angles $\chi1$ and $\chi2$ of Trp243 in the unoccupied receptor. Most of the time $\chi1$ stays between –60° and –90° (g+ conformation), but for about 1 ns this angle changes to *trans*. Apart from this prolonged conformational change, many short-lived switches to *trans* can be observed. Figure 9 shows the torsional angles of Trp243 in the receptor together with an inverse agonist. Comparing both graphs it is obvious that the presence of an inverse agonist stabilizes the starting conformation of Trp243. Not only was the conformational change suppressed, but also the overall fluctuation was reduced. The $\chi1$ value never drops below –150°. Finally, in Fig. 10 the torsional angels of Trp243 are shown in the presence of an agonist. After 2–3 ns the $\chi1$ angle changes to *trans*. In contrast to the unoccupied receptor it stays in this conformation for the rest of the simulation.

Figure 11 shows the Trp243 sidechain superimposed over the backbone atoms. During the equilibration the $\chi2$ value changed from 120° (green) to –30° (blue). This second conformation was stabilized by PSB-10 during the simulation. The presence of the agonist Cl-IB-MECA in the binding pocket resulted in the conformational change of $\chi1$ of Trp243 (yellow).

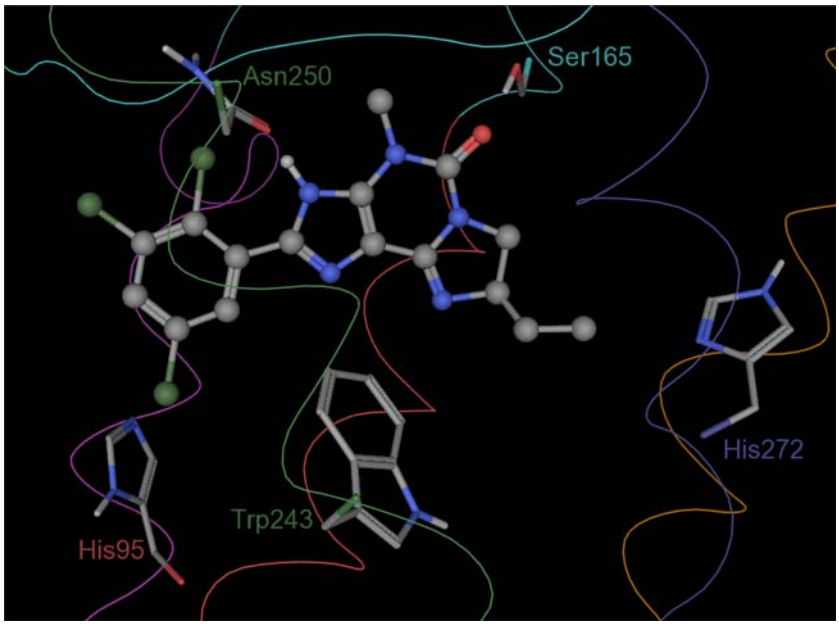

Fig. 6 Inverse agonist PSB-10 docked into the binding pocket of the hA_3 receptor (Color-coding: TM1: dark yellow, TM2: orange, TM3: dark red, TM4: magenta, TM5: light green, TM6: dark green, TM7 blue)

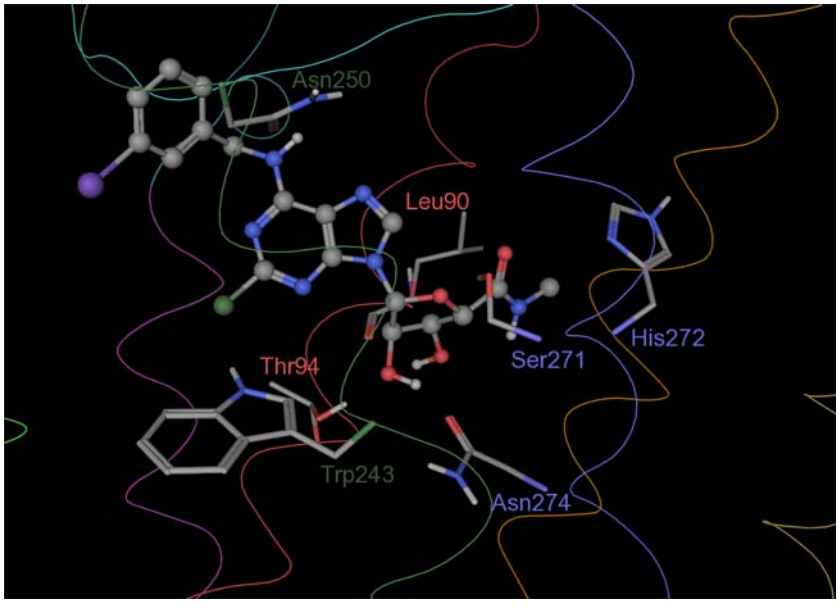

Fig. 7 Agonist Cl-IB-MECA docked into the binding pocket of the putative active conformation of the hA_3 receptor (Colour-coding: TM1: dark yellow, TM2: orange, TM3: dark red, TM4: magenta, TM5: light green, TM6: dark green, TM7 blue)

This observation is in good agreement with recent solid-state NMR measurements of the metarhodopsin II intermediate [31]. Crocker et al. concluded that the $Trp265^{6.48}$ side-chain moves towards TM5 and the $\chi 1$ torsion angle changes to *trans*. Further hints regarding this amino acid came from UV absorbance studies which showed that the plane of the indole side-chain of $Trp265^{6.48}$ in bovine rhodopsin tilts towards the membrane plane during activation [32].

The conformational change of $Trp243^{6.48}$ might be interpreted as an indication of the beginning activation process. The unoccupied receptor stays most of the time in an inactive conformation (Trp243: g+ conformation), but may spontaneously change into an active conformation (Trp243: *trans* conformation). This is in good agreement with the observed basal activity of GPCRs in the absence of agonists [33]. Inverse agonists do not only prevent agonists from activating the receptor but also stabilize the inactive receptor conformation. Finally, agonists are expected to have a distinct higher affinity to the active receptor conformation. Figures 12 and 13 show the measured interaction energies between the protein and PSB-10 and Cl-IB-MECA, respectively. Both Lennard-Jones and

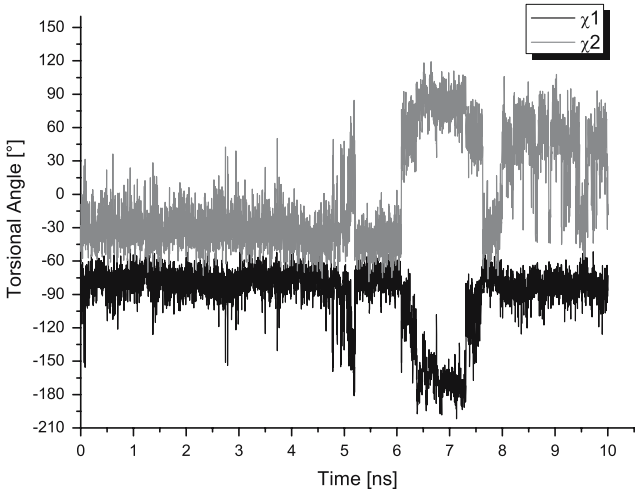

Fig. 8 Torsional angles $\chi 1$ and $\chi 2$ of Trp243 (unoccupied receptor) plotted versus time

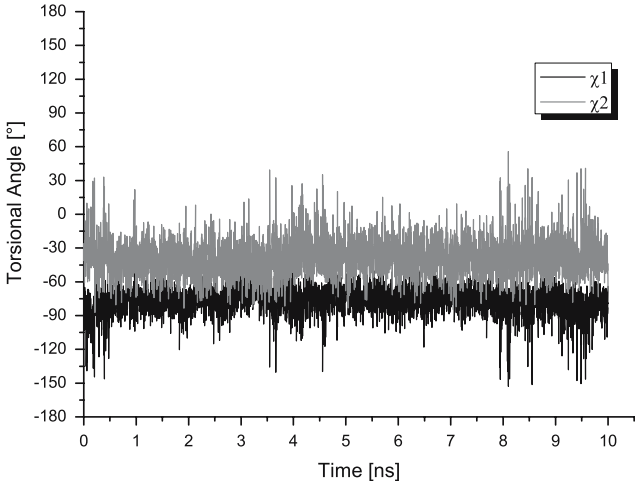

Fig. 9 Torsional angles $\chi 1$ and $\chi 2$ of Trp 243 (receptor together with PSB-10) plotted versus time

Coulomb energies are shown. Apart from an initial decline in energy in the simulation with PSB-10, no other significant change in the Lennard-Jones energy could be observed. This decline can be attributed to a slightly unfavourable placement of this ligand. In Fig. 13 a small, but statistically significant, change in the Coulomb energy could be observed at 3 ns. The time of this change correlates with the time of the conformational change of Trp243. The average electrostatic energy drops from –39.67 ± 9.21 to –49.77 ± 14.24. Such a change in Coulomb interaction energies can be attributed to the better accessibility of some polar amino acids (e.g. Ser271 and Asn274) after Trp243 adopts the *trans* conformation. The polar ribose moiety of Cl-IB-MECA may now form

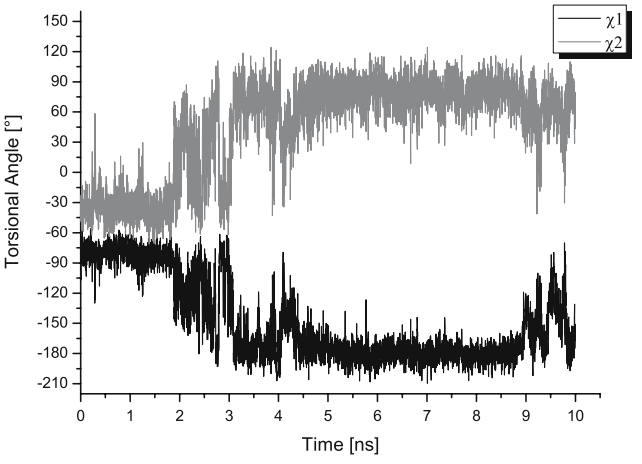

Fig. 10 Torsional angles $\chi 1$ and $\chi 2$ of 243 (receptor together with Cl-IB-MECA) plotted versus time

hydrogen bonds with those amino acids more easily. This gain in interaction energy may be responsible for the stabilization of the active conformation, after the spontaneous change of the receptor.

Ligand–protein interactions

We investigated the interactions between the ligands and the protein during the molecular dynamics simulation. Figure 14 shows the initial protein–Cl-IB-MECA complex and Fig. 15 after 10 ns. Before the simulation the agonist had only a few hydrogen bonding partners: Tyr254 and maybe Trp243 or Ser275 (hydrogen—acceptor distance >3Å). After the 10ns simulation Cl-IB-MECA has more possibilities for hydrogen bonding: Tyr254, Asn250, Ser271 and maybe Ser165 (hydrogen—acceptor distance >3Å) or even His272 (hydrogen—acceptor distance >4Å) and it moved a bit more to the extracellular side in the binding pocket. The shortest distance between Cl-IB-MECA and Trp243 increased from 3.1 Å to 4.4 Å. The hydrogen bond to Ser271 is probably the most important one. Before the molecular dynamics simulation Ser271 stabilized a kink in TM6, but after 10 ns it slightly changed its position to form a hydrogen bond to the 3′-OH group in Cl-IB-MECA (Fig. 16). This interruption of a stabilizing hydrogen bond may be responsible for the later movement of TM6 during the activation process.

PSB-10 started with two hydrogen bonds to Tyr254 and Ser165 (Fig. 17). In contrast to Cl-IB-MECA PSB-10 moved deeper into the binding pocket and thereby lost its hydrogen bond to Tyr254, but established a close contact with Trp243. It formed a hydrogen bond and a π–π interaction between the phenyl moiety and

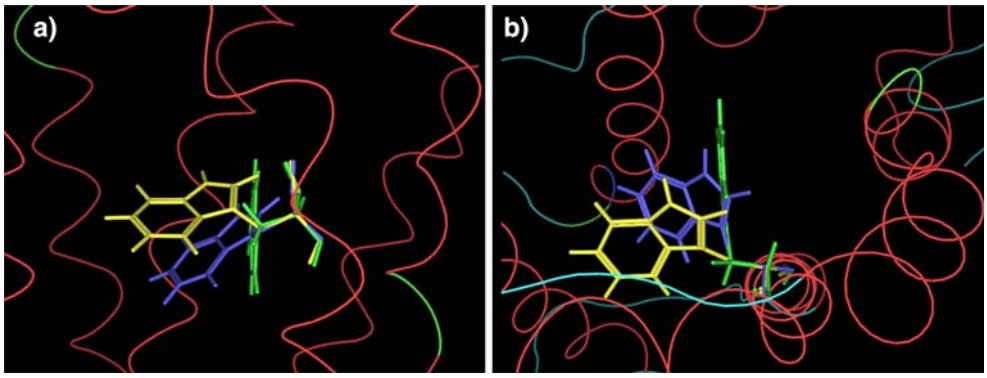

Fig. 11 Trp243 sidechain superimposed over the backbone atoms viewed from the membrane plane (**a**) and from the extracellular side (**b**). Conformation before molecular dynamics simulation (green), after simulation together with PSB-10 (blue) and after simulation together with Cl-IB-MECA (yellow)

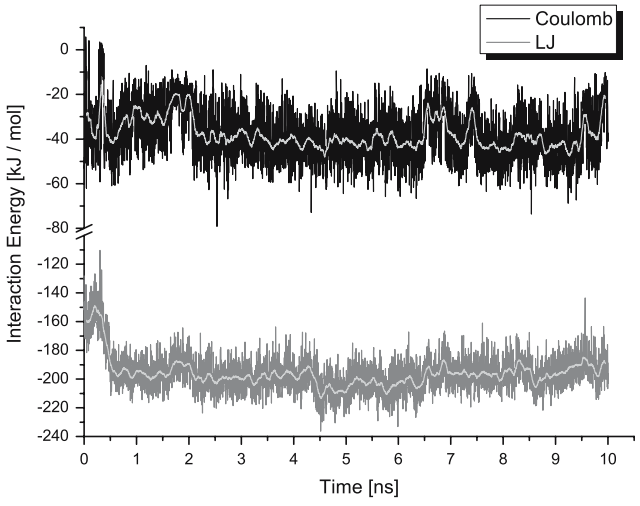

Fig. 12 Interaction energies between the protein and PSB-10 plotted versus time. Light grey line shows the average energy over 100 ps

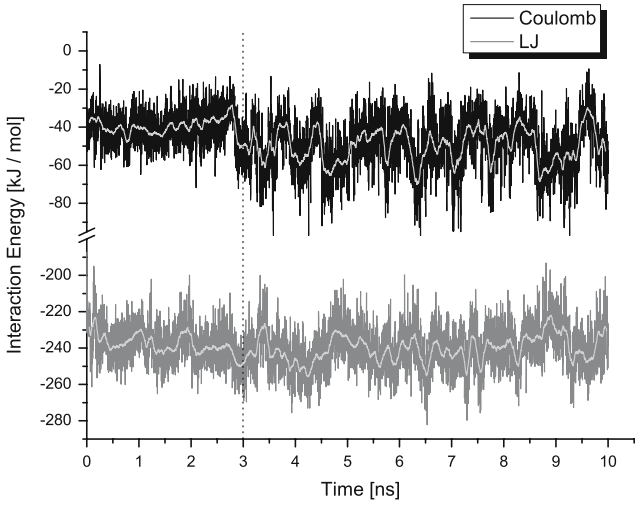

Fig. 13 Interaction energies between the protein and Cl-IB-MECA plotted versus time. Light grey line shows the average energy over 100 ps

the indole moiety of Trp243 (Fig. 18). The distance between the nitrogen in the indole moiety of Trp243 and the closest nitrogen in PSB-10 decreased from 7.3 Å to 3.0 Å. The shortest distance between the trichlorophenyl group and the indole moiety decreased from 5.0 Å to 3.5 Å. This close contact stabilized Trp243 and impeded a conformational change.

Movement and rotation of TM6 upon receptor activation

In order to investigate whether the predicted movement of TM6 could be observed, we measured certain changes in inter-atomic distances. As points of reference we chose three α-carbon atoms in each TM domain (extra- and intracellular side, and in the middle). These atoms are listed in Table 1. The α-carbons in TM 3, 5 and 7 are all facing TM6. The chosen α-carbons in TM6 are facing TM3. Therefore counterclockwise rotation of TM6 would result in a decreased inter-atomic distance between TM5 and TM6, in conjunction with a large increase between TM7 and TM6 and a moderate increase between TM3 and TM6. Movement of TM6 away from TM3 would (obviously) result in an increased distance between these two TM domains, in conjunction with a moderate increase in distances to both TM5 and TM7.

In Table 2 the measured inter-atomic distances are shown. No significant differences exist between the distances in the molecular dynamics simulations performed in the presence of an agonist or inverse agonist. Also inspection of each inter-atomic distance plotted against time revealed no discernible trend (data not shown).

Figure 19 shows the Root Mean Square Fluctuation plot (RMSF plot) calculated for all individual residues. As expected differences in the RMSF plot are only small. But maybe the RMSF plot of the residues in the intracellular part of TM6 is noteworthy. In the molecular dynamics simulation with an agonist the

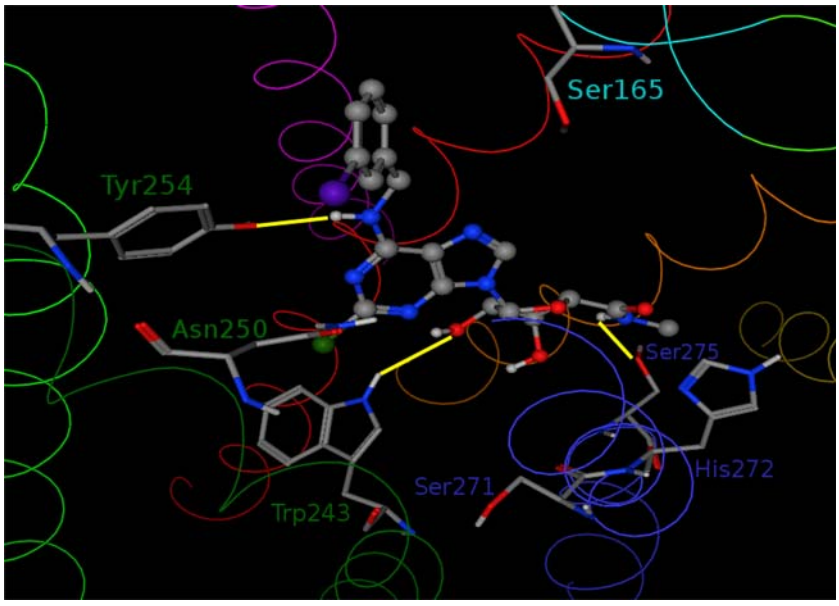

Fig. 14 Protein–Cl-IB-MECA complex before molecular dynamics simulation viewed from the extracellular side. Potential hydrogen bonds are shown as yellow lines

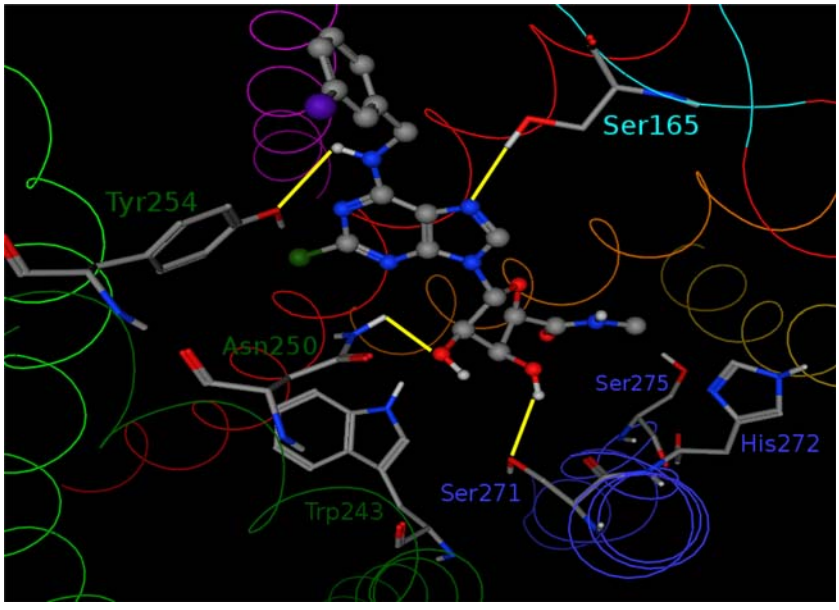

Fig. 15 Protein–Cl-IB-MECA complex after 10 ns of molecular dynamics simulation viewed from the extracellular side. Potential hydrogen bonds are shown as yellow lines

fluctuation is higher compared to the one with an inverse agonist or the unoccupied receptor. The actual movement could not be detected, but the higher fluctuation may indicate a destabilizing effect of an agonist in this region of the protein. In addition the average RMSF values are slightly higher in a simulation with an agonist (0.090 nm) compared to the simulation with PSB-10 (0.085 nm) and the unoccupied receptor (0.087 nm).

So unfortunately, no more of the predicted conformational changes occurred during the molecular dynamics simulation. Neither a rotation of TM6 nor an increased distance between the cytoplasmic ends of TM6 and TM3 could be observed. This may have several reasons. First, we only simulated 10 ns in the presence of an agonist. Rhodopsin is known for its quick response but the activation process nevertheless takes time in the millisecond range [34]. For the β2-receptor an activation time of several minutes was measured [35]. At present such a long simulation would take thousands of years. Second, protonation of the aspartic/glutamic acid in the D/E RY motif is assumed to play an important role in the activation process [33]. Unfortunately, molecular dynamics simulations based on force field calculations cannot imitate a proton uptake. Bonds can not be broken nor created. This limitation may be overcome with the application of the QM/MM molecular dynamics

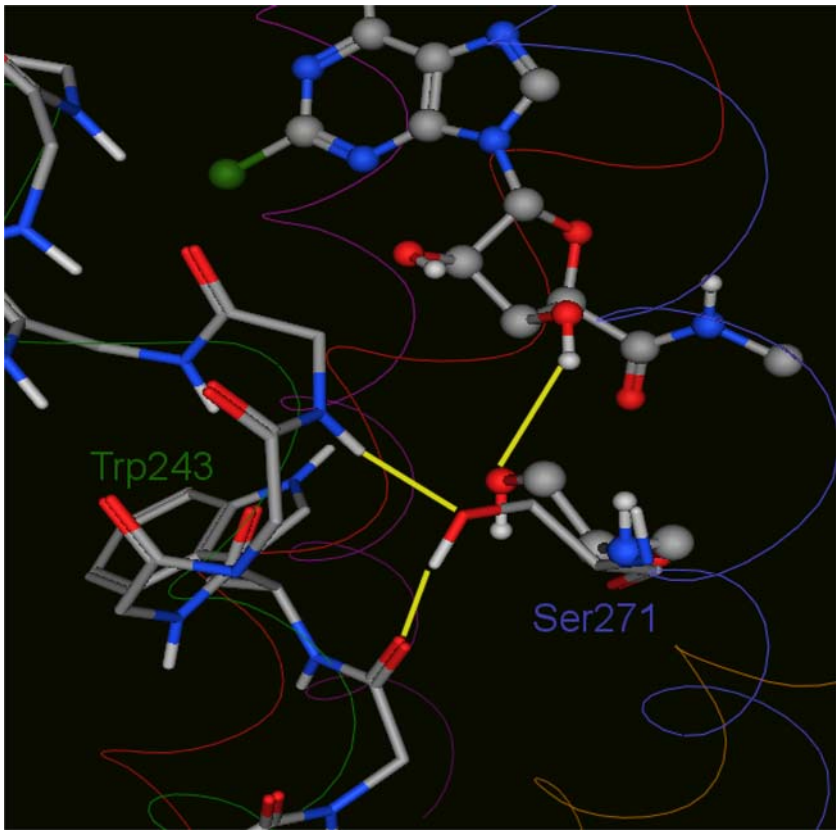

Fig. 16 Hydrogen bonds of Ser271 before (sticks) and after (balls and sticks) molecular dynamics simulation of the hA_3 receptor together with Cl-IB-MECA

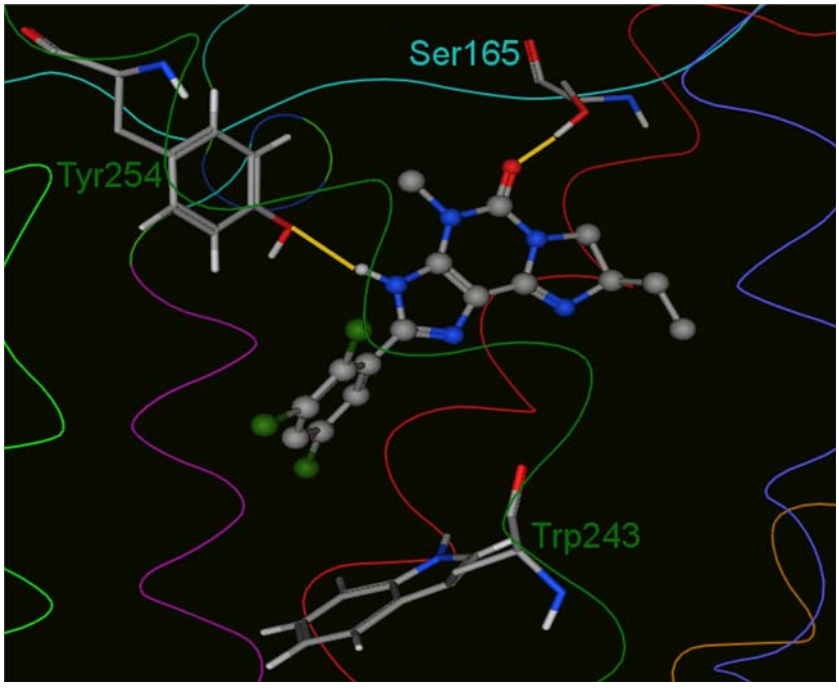

Fig. 17 Protein–PSB-10 complex before molecular dynamics simulation viewed from the membrane plane. Potential hydrogen bonds are shown as yellow lines

method [36]. On the pre-condition that the time-costly quantum mechanical calculations are applied only to certain known regions this method is feasible.

Third, the G-Protein was not included in this simulation. It is known that the G-Protein has a significant influence on the state of the receptor, e.g., addition of GTP results in an increased affinity of agonists to GPCRs. The G-Protein is quite large (47 kDa) compared to the hA_3 receptor (38 kDa). Inclusion of the G-Protein would have resulted in a far bigger

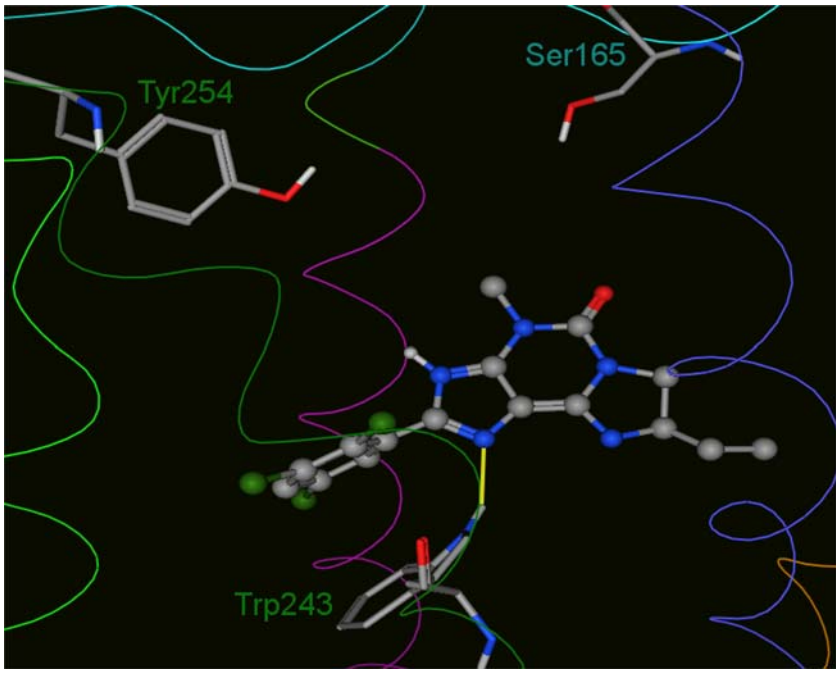

Fig. 18 Protein–PSB-10 complex after 10 ns of molecular dynamics simulation viewed from the membrane plane. Potential hydrogen bonds are shown as yellow lines

Table 1 Atoms selected for measurement of inter-atomic distances

TMD	Cα of	Position
3	Phe80	Extracellular
3	Thr94	Middle
3	Arg108	Intracellular
5	Asp175	Extracellular
5	Ile186	Middle
5	Ille200	Intracellular
6	Tyr254	Extracellular
6	Trp243	Middle
6	Thr228	Intracellular
7	Leu264	Extracellular
7	Ser271	Middle
7	Ille286	Intracellular

Table 2 Average distances measured between TM6 and TM 3, 5, and 7

Distance between	Position	Cl-IB-MECA simulation	PSB10 simulation
TM3–TM6	Extracellular	20.4 ± 0.50	20.4 ± 0.61
	Middle	10.1 ± 0.49	10.6 ± 0.38
	Intracellular	8.4 ± 0.33	8.6 ± 0.40
TM5–TM6	Extracellular	7.9 ± 0.31	7.6 ± 0.34
	Middle	11.6 ± 0.50	11.8 ± 0.45
	Intracellular	10.3 ± 0.45	10.3 ± 0.41
TM7–TM6	Extracellular	12.3 ± 0.32	12.7 ± 0.41
	Middle	5.1 ± 0.31	5.1 ± 0.29
	Intracellular	7.3 ± 0.50	7.2 ± 0.42

simulation box and an dramatically increased computation time. Furthermore the exact points of interaction between the GPCRs and the G-Proteins are unknown. Therefore we had no other choice but to omit the G-Protein in our calculations.

Finally, the composition of the phospholipid bilayer was observed to play an important role in the activation process of rhodopsin [37, 38]. Till now, no membrane model exists with a natural lipid composition (phosphatidylcholine, phosphatidylserine, phosphatidylethanolamine, and polyunsaturated fatty acyl chains).

Conclusion

We were able to identify conformational changes of Trp243 depending on receptor occupation. These changes are in good agreement with experimental results from NMR and UV studies. In the case of the hA_3-receptor a gain in electrostatic interaction energy may be responsible for the stabilization of the *trans* conformation of $Trp243^{6.48}$.

Due to current limitations of computer performance and/or simulation methods no further conformational changes could be observed. Nevertheless, the first results suggest that homology models based on the crystal structure of rhodopsin may be appropriate tools to investigate the activation process of GPCRs. There is reasonable hope that advanced techniques (e.g., QM/MM) applied to molecular dynamics studies can help to achieve a better understanding of the activation process of GPCRs.

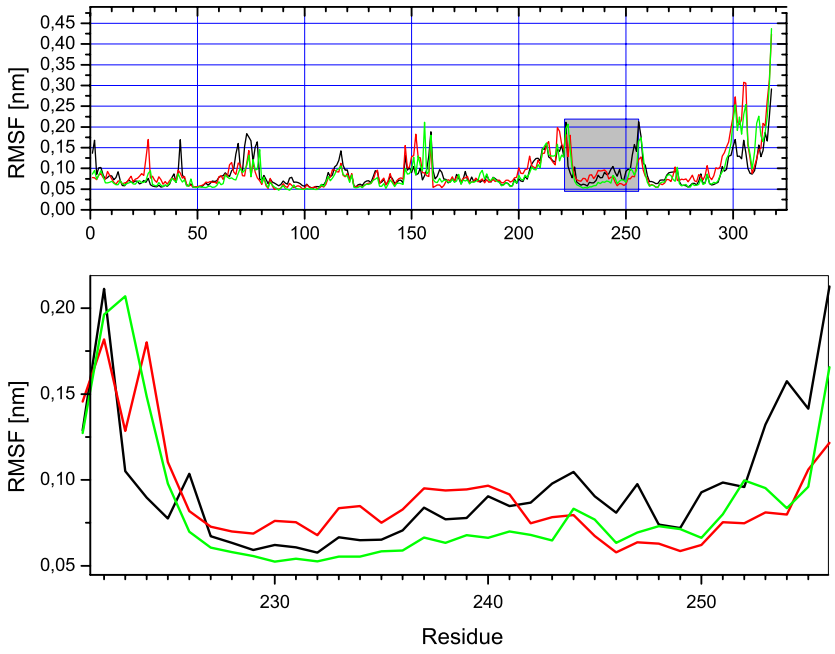

Fig. 19 RMSF plot calculated for all individual residues of the hA3 receptor. The lower plot shows only the RMSF plot of TM6. (Colour-coding: unoccupied receptor: black; receptor & Cl-IB-MECA: red; receptor & PSB-10: green)

References

1. Filmore D (2004) Mod Drug Discov 7:24
2. Palczewski K, Kumasaka T, Hori T, Behnke CA, Motoshima H, Fox BA, Le TI, Teller DC, Okada T, Stenkamp RE, Yamamoto M, Miyano M (2000) Science 289:739
3. Okada T, Ernst OP, Palczewski K, Hofmann KP (2001) Trends Biochem Sci 26:318
4. Duprez L, Parma J, Costagliola S, Hermans J, Van SJ, Dumont JE, Vassart G (1997) FEBS Lett 409:469
5. Nanevicz T, Wang L, Chen M, Ishii M, Coughlin SR (1996) J Biol Chem 271:702
6. Allen LF, Lefkowitz RJ, Caron MG, Cotecchia S (1991) Proc Natl Acad Sci USA 88:11354
7. Kjelsberg MA, Cotecchia S, Ostrowski J, Caron MG, Lefkowitz RJ (1992) J Biol Chem 267:1430
8. Arnis S, Fahmy K, Hofmann KP, Sakmar TP (1994) J Biol Chem 269:23879
9. Scheer A, Fanelli F, Costa T, De Benedetti PG, Cotecchia S (1996) EMBO J 15:3566
10. Rasmussen SG, Jensen AD, Liapakis G, Ghanouni P, Javitch JA, Gether U (1999) Mol Pharmacol 56:175
11. Scheer A, Fanelli F, Costa T, De Benedetti PG, Cotecchia S (1997) Proc Natl Acad Sci USA 94:808
12. Han M, Smith SO, Sakmar TP (1998) Biochemistry 37:8253
13. Javitch JA, Fu D, Liapakis G, Chen J (1997) J Biol Chem 272:18546
14. Farrens DL, Altenbach C, Yang K, Hubbell WL, Khorana HG (1996) Science 274:768
15. Patel AB, Crocker E, Eilers M, Hirshfeld A, Sheves M, Smith SO (2004) Proc Natl Acad Sci USA 101:10048
16. Jager F, Jager S, Krutle O, Friedman N, Sheves M, Hofmann KP, Siebert F (1994) Biochemistry 33:7389
17. Nakayama TA, Khorana HG (1991) J Biol Chem 266:4269
18. Jonathan JR, Mielke T, Vogel R, Villa C, Schertler GFX (2004) EMBO 23:3609
19. Gao ZG, Chen A, Barak D, Kim SK, Muller CE, Jacobson KA (2002) J Biol Chem 277:19056
20. Okada T, Fujiyoshi Y, Silow M, Navarro J, Landau EM, Shichida Y (2002) Proc Natl Acad Sci USA 99:5982
21. Kehraus S, Gorzalka S, Hallmen C, Iqbal J, Muller CE, Wright AD, Wiese M, Konig GM (2004) J Med Chem 47:2243
22. Schuttelkopf AW, van Aalten DM (2004) Acta Crystallogr D Biol Crystallogr 60:1355
23. Kim J, Jiang Q, Glashofer M, Yehle S, Wess J, Jacobson KA (1996) Mol Pharmacol 49:683
24. Olah ME, Jacobson KA, Stiles GL (1994) J Biol Chem 269:24692
25. Shi L, Javitch JA (2002) Annu Rev Pharmacol Toxicol 42:437
26. Buller S, Zlotos DP, Mohr K, Ellis J (2002) Mol Pharmacol 61:160
27. Voigtlander U, Johren K, Mohr M, Raasch A, Trankle C, Buller S, Ellis J, Holtje HD, Mohr K (2003) Mol Pharmacol 64:21
28. Klotz KN, Camaioni E, Volpini R, Kachler S, Vittori S, Cristalli G (1999) Naunyn Schmiedebergs Arch Pharmacol 360:103
29. Ozola V, Thorand M, Diekmann M, Qurishi R, Schumacher B, Jacobson KA, Muller CE (2003) Bioorg Med Chem 11:347
30. Kim SK, Gao ZG, Jeong LS, Jacobson KA (2006) J Mol Graph Mod 25:562
31. Crocker E, Eilers M, Ahuja S, Hornak V, Hirshfeld A, Sheves M, Smith SO (2006) J Mol Biol 357:163
32. Lin SW, Sakmar TP (1996) Biochemistry 35:11149
33. Gether U (2000) Endocr Rev 21:90
34. Borhan B, Souto ML, Imai H, Shichida Y, Nakanishi K (2000) Science 288:2209
35. Gether U, Kobilka BK (1998) J Biol Chem 273:17979
36. Lee YS, Krauss M (2004) J Am Chem Soc 126:2225
37. Gibson NJ, Brown MF (1993) Biochemistry 32:2438
38. Wiedmann TS, Pates RD, Beach JM, Salmon A, Brown MF (1988) Biochemistry 27:6469